

## A gelation analogy of crustal formation derived from fractal conductive structures

Karsten Bahr,<sup>1,2</sup> Maxim Smirnov,<sup>3</sup> Erich Steveling,<sup>4</sup> and BEAR Working Group<sup>5</sup>

Received 7 March 2001; revised 28 April 2002; accepted 5 May 2002; published 21 November 2002.

[1] The statistical evaluation of numerical random media models and of electromagnetic array data provides evidence of fractal conductive structures in the middle and lower crust. During the search for an electrical conduction mechanism that is compatible with the geophysical anomalies in the middle and lower crust, random resistor networks were developed. These networks contain two types of resistors, representing the rock matrix and the conductive phase. Here we demonstrate that random resistor network models can also explain the statistical properties of the electric field distortion measured in large-scale electromagnetic array experiments. Correspondence between measured and modeled distortion statistics is obtained if the structures formed by the two resistor types in the networks have a fractal geometry. This can indicate that the natural conductive networks also have a fractal geometry and stay close to a percolation threshold. A simple scale model of crust formation mechanics is considered in order to find an analog medium and an analog process that creates such a geometry. We suggest gelation as a rheological analogy that allows for a coexistence of ductile and brittle behavior of material in the lower crust. This process forms fractal structures in the host matrix and fractal conductive networks, provided that conductive material is available at that time of crustal evolution. The statistical evaluation of the field data provides evidence for a fractal structure with an upper bound of the size of Fennoscandia. *INDEX TERMS*: 0659 Electromagnetics: Random media and rough surfaces; 1020 Geochemistry: Composition of the crust; 1515 Geomagnetism and Paleomagnetism: Geomagnetic induction; 1848 Hydrology: Networks; 3250 Mathematical Geophysics: Fractals and multifractals; *KEYWORDS*: lower crust, conduction mechanism, resistor networks, electric field distortion, gelation

**Citation:** Bahr, K., M. Smirnov, E. Steveling, and BEAR Working Group, A gelation analogy of crustal formation derived from fractal conductive structures, *J. Geophys. Res.*, 107(B11), 2314, doi:10.1029/2001JB000506, 2002.

### 1. Introduction

[2] The lower continental crust is generally referred to as a weak layer that can transfer stress between the brittle upper crust and the mantle via ductile flow [Kruse *et al.*, 1991; Kaufmann and Royden, 1994]. It has caught the imagination of many earth scientists because of the controversies about its composition and physical state. Electromagnetic (EM) field studies yielded strong evidence for electrical conductors in the lower crust [e.g., Jones, 1992], at depths below 12–13 km in Northern Bavaria [Bahr *et al.*, 2000] and deeper than 25 km in Finland [Korja and Hjelt, 1993]. A significant fraction of recent electromagnetic literature advocates saline fluids trapped at the brittle-ductile

transition to be the origin of these conductors [e.g., Bailey *et al.*, 1989]. This view was challenged both with geophysical arguments that claim that the conductors can also originate from an electronic conduction mechanism [e.g., Mareschal *et al.*, 1992] and with petrological arguments claiming that the lower crust has to be dry [e.g., Yardley and Valley, 1997]. This debate is not finished yet as indicated by the recent exchange between Wannamaker [2000], who advocates fluids, and Yardley and Valley [1997, 2000], who advocate a dry lower crust.

[3] The “wet” lower crust model is supported by geophysicists who argue that it can explain the occurrence of both reflectivity and electrical conductors [Marquis and Hyndman, 1992; Merzer and Klempner, 1992]. However, recent work by Simpson and Warner [1998] indicates that the two geophysical anomalies do not always occur in the same depth ranges. While fluids might play an important role in the conduction mechanism in active tectonics regimes and in the genesis of magmas, a strong geophysical point against the fluid paradigm was made by a quantitative evaluation of electrical anisotropy in electromagnetic array data from geologically old, stable areas [Bahr *et al.*, 2000; Simpson, 2001]. Bulk anisotropy only occurs for a low degree of interconnectivity of the highly conducting phase

<sup>1</sup>Geology and Geophysics, Adelaide University, Adelaide, South Australia, Australia.

<sup>2</sup>Now at Institut für Geophysik, Universität Göttingen, Göttingen, Germany.

<sup>3</sup>Institute of Physics, St. Petersburg University, St. Petersburg, Russia.

<sup>4</sup>Institut für Geophysik, Universität Göttingen, Göttingen, Germany.

<sup>5</sup>Geological Survey of Finland, Espoo, Finland.

[Bahr, 1997], and therefore the amount of conducting material must be significantly larger than estimated from simple mixing laws for the case of perfect interconnection [e.g., Waff, 1974]. However, in addition to bulk anisotropy also structurally controlled electrical anisotropy has been found, and a link between the degree of anisotropy and the amount of conductive material cannot be made in these cases. An example is the large anisotropy found in hand samples from a former terrane boundary [Jones *et al.*, 1997]. However, because anisotropy is also found in magnetotelluric field data from sites far away from terrane boundaries (the distance is larger than the electromagnetic penetration depth), it can not only be related geologically controlled anisotropy at terrane boundaries or other elongated structures.

[4] Resistor networks were first used by Madden [1976] to understand the conduction mechanism in heterogeneous media and by Kemmerle [1977] to explain the distortion imposed on the electric field by small-scale surface scatterers. Embedded networks were employed by Madden [1976] in order to describe very large two-phase systems, and by Bahr [1997] for explaining two aspects of the conduction mechanism in EM field data: conductivity distribution functions and anisotropy of the electrical conductivity with respect to two horizontal directions. If slightly more resistors representing the conductive phase occur in one direction, then bulk conductivity anisotropy is created. The fractal geometry was imposed on these networks because they were embedded networks, and the original reason for choosing this geometry was the reduced computational power required for calculating the conductances of embedded networks: the currents in small-scale networks can be calculated analytically or with a small equation system. The solution for the embedded network is then assembled from the solutions of the subnetworks. Labendz [1999] and Bahr [2000] performed numerical random resistor experiments with large nonembedded networks. Bahr [2000] provides the equations that have to be solved in order to find the current distribution within the network. For two-dimensional bond percolation, at the percolation threshold the resistors representing the conductive phase have a fractal geometry. The fractal geometry can be found with the technique of cluster counting [e.g., Stauffer and Aharony, 1992]. The numerical experiments by Labendz [1999] and Bahr [2000] in which the fractal geometry was not imposed on the networks anymore reproduced the bulk conductivity anisotropy.

[5] In this paper we show how partly interconnected and possibly self-similar networks of conductive material can be found in the crust with electromagnetic sounding techniques. Rather than discussing the conduction mechanism the distortion of electric fields in EM array data is considered. In section 2 we demonstrate for a particular data set how the distortion can be described by statistical measures such as distortion variance and frequency distribution functions of the distortion amplitude. We then show that large random resistor networks can be employed to reproduce these statistical properties of the EM field data numerically. Finally, we extend earlier analogue models of crustal formation in an attempt to show that gelation can be an analogy of a crustal formation which generates self-similar structures. Although the proposed gelation analogy must clearly be marked as a hypothesis, it might also explain the

survival of conductive networks over geological times, in the presence of ductile flow in the lower crust.

## 2. Heterogeneity of Voltage Variations in Field Data

[6] Many contributions to electromagnetic (EM) literature in the 1980s and early 1990s were devoted to the removal of “distortion”: the influence of small-scale scatterers on the magnetotelluric impedance tensor prior to forward modeling or inversion (e.g., review by Groom and Bahr [1992]). This “two-step interpretation” was necessary because most modeling schemes can not handle crustal or upper mantle conductivity anomalies (on 10–100 km scale length) and small-scale (<1 km) scatterers simultaneously due to limited grid size and resolution.

[7] In this section, we describe the distortion in electromagnetic data collected at 40 sites during summer 1998 in the Baltic Electromagnetic Array Research (BEAR) project [Korja and BEAR Working Group, 2000] in Scandinavia, in order to derive a statistical model of distortion. The distortion caused by a heterogeneous scatterer is described by a distortion tensor. It links the normal electric field  $E_n$  that would be measured in the absence of the scatterer, to the measured electric field

$$\mathbf{E} = \begin{pmatrix} a_{11} & a_{12} \\ a_{21} & a_{22} \end{pmatrix} \mathbf{E}_n. \quad (1)$$

The elements of the distortion tensor can alternatively displayed as skew angles  $\beta_1, \beta_2$  defined by

$$\tan \beta_1 = -a_{12}/a_{22}, \quad \tan \beta_2 = a_{21}/a_{11}, \quad (2)$$

and as scaling coefficients  $s_1, s_2$  defined by

$$s_1 = (a_{12}^2 + a_{22}^2)^{1/2}, \quad s_2 = (a_{21}^2 + a_{11}^2)^{1/2}. \quad (3)$$

The skew angles can be determined from the measured impedance tensor but the scaling coefficients can only be estimated if an undistorted reference impedance is available [Groom and Bahr, 1992]. Bahr [2000] explained the skew angles and the appearance of very large scaling coefficients by the action of a percolation network on the long-period electromagnetic field, but the statistical properties of EM field data were not considered in that approach.

[8] From the distribution of the EM field sites in the BEAR project (Figure 1), it is obvious that a conventional conductivity model for the 20–60 km depth range can not be obtained from these data. The site spacing of 120 km exceeds the depth of the target and therefore spatial aliasing would occur. For the same reason, anisotropic conduction cannot be resolved. However, the distortion which inhomogeneous conductors in the middle crust impose on long-period (10,000 s) electromagnetic fields can be evaluated in a statistical sense in order to describe the heterogeneity of those conductors. The 10,000 s period has been chosen for three reasons: (1) a reference impedance from geomagnetic transfer functions [Schmucker, 1973]) is available at this and at longer periods. (2) The penetration depth of the electromagnetic field at 10,000 s, 250 km, exceeds the depth of the midcrustal conductor by a factor of 8–10 and therefore the

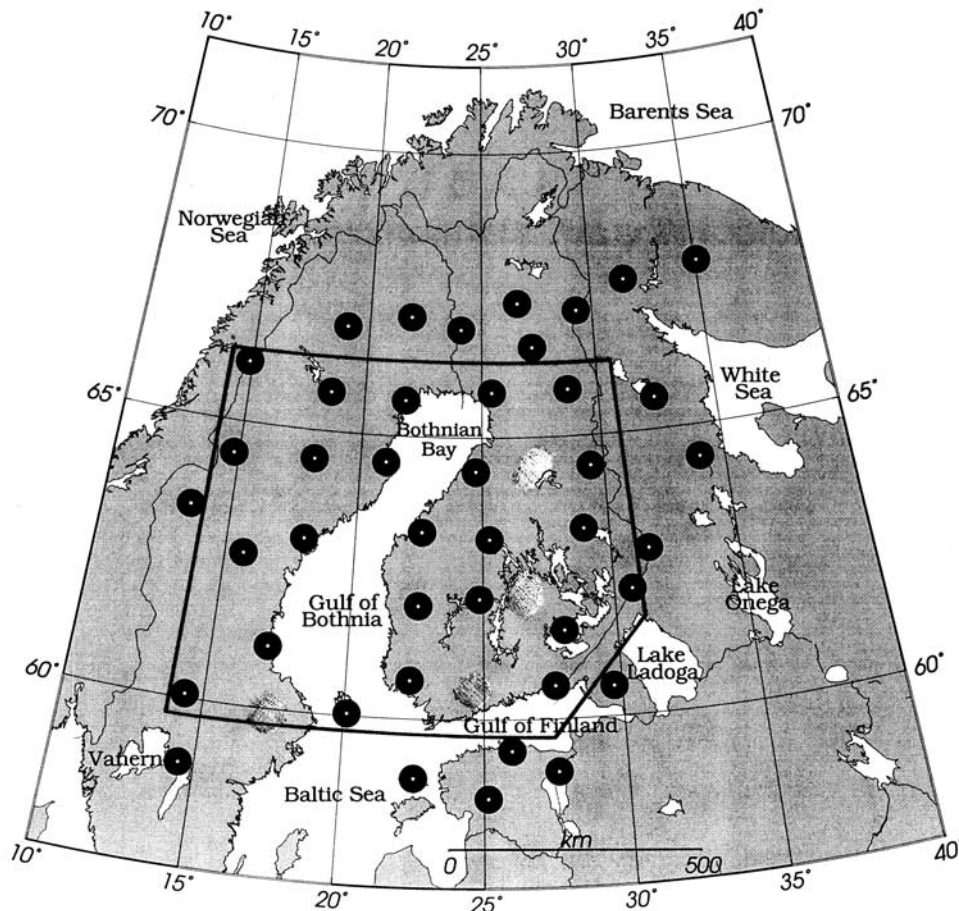


**Figure 1.** BEAR (Baltic Electromagnetic Array Research) field sites. The 24 central sites for which field data are presented in Figure 2 are marked with a box.

assumption that an heterogeneous midcrustal conductor acts like a galvanic scatterer, rather than in an inductive manner, is justified. A field data example for this effect is presented by *Bahr et al.* [2000, Figure 5]: At long periods above 3000 s, the phase split associated with crustal heterogeneity vanishes but the amplitude split does not. (3) Despite the high geomagnetic latitude of the target area there are still enough data segments in which the plane wave assumption is not violated [*Smirnov et al.*, 2000; *Sokolova et al.*, 2000] for this period and for shorter periods.

[9] Correct magnetotelluric depth estimations are hindered by local distortions of the electric field amplitudes due to crustal heterogeneities. These distortions have been corrected using magnetic transfer functions derived from the daily fluctuations of the magnetic field generated by current vortices in the ionosphere [*Schmucker, 1973; Bahr et al., 2000*]. However, electromagnetic source field heterogeneities [*Osipova et al.*, 1989] hinder estimation of electromagnetic transfer functions at periods above 10,000 s in Scandinavia, rendering this correction technique inapplicable. Therefore we used one-dimensional conductivity models of the 200–600 km depth range including a conductivity increase at the olivine-wadsleyite transition at 410-km depth, which is visible both in laboratory and field data of mantle conductivity [*Xu et al., 2000; Bahr and Duba, 2000*] in order to calculate a reference impedance at the 10,800 s period. The use of a one-dimensional reference impedance

is justified at periods as long as 10,000 s, because the electromagnetic fields at these periods penetrate deep into both the continental and the oceanic mantle. At much shorter periods these penetration depths are dominated by the resistive continental lithosphere and the conductive seawater, respectively. Then an adjustment effect [*Raganayaki and Madden, 1980*] due to the ocean-continent contact at the shelf edge in the Norwegian sea can make the reference impedance “anisotropic” with respect to the orientation of the shelf edge.

[10] By comparing the measured impedance tensor at each site to the reference impedance, we obtain the distortion tensor for each site. This comparison technique has been described by *Bahr et al.* [2000], and the Schmucker-Weidelt transfer function [*Schmucker, 1973*] calculated from that reference impedance at the period 10,800 s is  $C = 272 \text{ km} - i 209 \text{ km}$ . Although conductors at all depths above 200 km can possibly contribute to the distortion, we assume that the structure in the middle crust provides the strongest contribution to the distortion for the following reasons: (1) Finnish audiomagnetotelluric data with penetration depths in the upper crust [*Korja, 1993*] show less spatial variability than the long-period data, and adjacent long-period sites show often similar distortion. (2) A detailed study which combined audiomagnetotelluric and long-period data from southern Germany proved the overwhelming distortion effect of the midcrustal structure [*Bahr et al., 2000*].

[11] For the central 24 sites of the BEAR array, the distortion is displayed in Figure 2. At each site the left column of the distortion tensor (equation (1)) is shown as distortion vector

$$\mathbf{s}_2 = a_{11}\hat{\mathbf{x}} + a_{21}\hat{\mathbf{y}}, \quad (4)$$

where  $\hat{\mathbf{x}}$  and  $\hat{\mathbf{y}}$  are unit vectors in north and east direction, respectively. If no distortion occurs, then  $a_{21} = 0$  as there is no skew angle and  $a_{11} = 1$  because there is no scaling. Obviously distortion in the target area is very heterogenous. This heterogeneity is also described by the frequency distribution of the overall scaling coefficients at each site

$$s = (a_{11}^2 + a_{22}^2 + a_{12}^2 + a_{21}^2)^{1/2} \quad (5)$$

in Figure 3 and by the distortion variance of the entire array

$$\text{Var} = \sum_{i=1}^N (s_i - \bar{s})^2 / (N - 1), \quad (6)$$

where  $N$  is the number of sites,  $s_i$  is the overall scaling at site  $i$  and  $\bar{s}$  is the average overall scaling in the array. For the  $N = 40$  sites of the BEAR array the average distortion is 3.1, the variance is 14.1, and the standard deviation is  $\sqrt{\text{Var}}/\sqrt{N} = 0.59$ . *Ogawa and Uchida* [1996] pointed out that the average distortion coefficients  $a_{11}$  and  $a_{22}$  should be 1 if the area around a scatterer is covered by many sites with a sufficiently small spacing. If no spatial aliasing occurs, then the average overall scaling coefficient (equation (5)) should therefore be  $\sqrt{2}$ . Our result can not contradict or support this hypothesis because spatial aliasing does occur due to the large site spacing in the BEAR array. Instead, the telluric distortion at these 40 sites is a random sample of the distortion that would be measured with a sufficiently dense spaced array. If we convert the standard

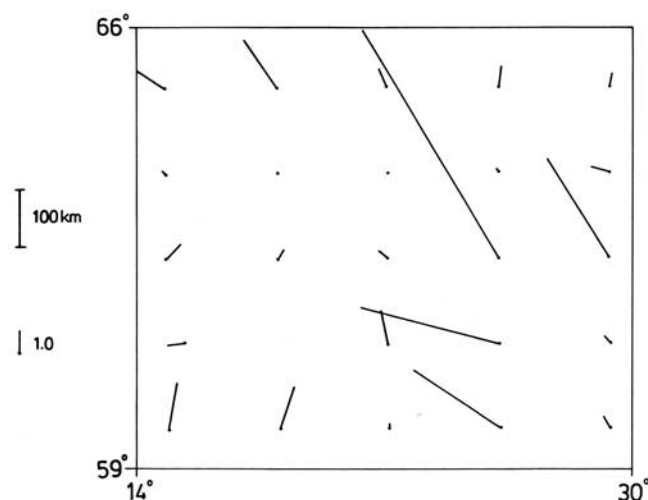


**Figure 2.** Distortion vectors according to equation (2), for 24 central sites of the BEAR array (see Figure 1). The spatial distribution of the field sites is less regular than in this display, but this display can be directly compared to a model data example in Figure 5.

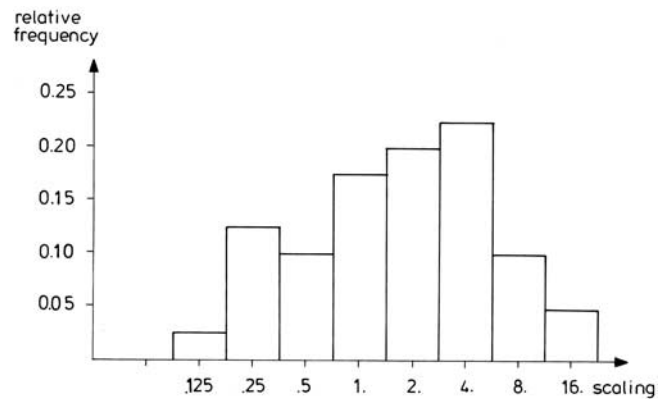


**Figure 3.** Frequency distribution of the dimensionless overall scaling coefficients according to equation (5) for 40 sites.

deviation into a 99% confidence limit, then our estimation of the average distortion is  $(3.1 \pm 1.77)$ , and the expected value  $\sqrt{2}$  is still within these limits. A change of the reference impedance would change the median of the overall scaling coefficient distribution in Figure 3 and could change the width of the curve but not its skewness. In order to demonstrate how strongly the analysis depends on the choice of a particular field data sample, we repeat the analysis without the two sites that exhibit the strongest distortion (see Figure 2), and then the average distortion is  $(2.4 \pm 1.15)$ .

### 3. Fractal and Nonfractal Random Resistor Networks: From Conduction to Voltage Variations

[12] Numerical random resistor network studies by *Bahr* [1997] and *Labendz* [1999] showed that bulk conductivity anisotropy can only occur if the network stays close to the percolation threshold in both directions; for example, for bond percolation in a two-dimensional network [*Bernasconi*, 1978], approximately 50% of the resistors should represent the conductive phase (Figure 4). If that fraction is much smaller than 50%, then no interconnectivity of the conductive material and therefore no bulk conductivity is found. If many more than 50% of the resistors represent the conductive phase in both directions, then similar bulk conductivities are found for both directions and no large anisotropy occurs. Cluster counting [e.g., *Stauffer and Aharony*, 1992] can prove that at the percolation threshold the conductive phase in Figure 4 has a fractal geometry. Can random resistor networks also be used to reproduce the statistical measures of the distortion in the field data presented in section 2?

[13] The distortion vectors at  $39^2 = 1521$  sites in one particular realization of a  $40 \times 40$  resistor network in the vicinity of the percolation threshold are plotted in Figure 5. This display of the distortion is directly comparable to the one in Figure 2 because the elements  $a_{11}$  and  $a_{21}$  of the distortion tensor are the normalized voltages [*Bahr*, 2000] at the resistors in  $x$  and  $y$  direction, respectively.

[14] The average distortion variance (equation (6)) is maximal at the percolation threshold, and for a  $40 \times 40$  resistor network this variance is 7.6 [*Bahr*, 2000]. The

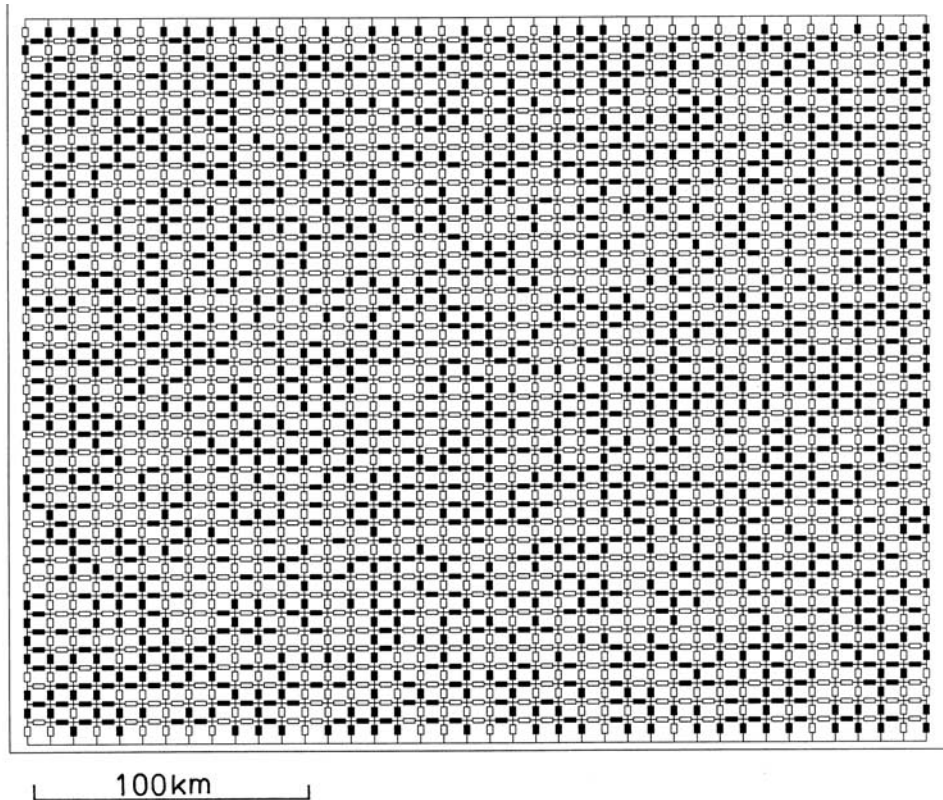


**Figure 4.** A realization of the  $40 \times 40$  resistor network at the percolation threshold for bond percolation. 50% of the resistors represent conductive material (solid resistor symbols) and 50% represent resistive material (open resistor symbols). Alternatively, this figure can also represent a fraction of a random realization of the virtual  $120 \times 120$  resistor network that emerges from the comparison of the distortion variances in field and model data (equations (6) and (7)). Then this is a map with a scale, but no spatial references are given because the “map” could be any  $320 \times 320$  km fraction of the lower crust of Fennoscandia.

variance in the field data, 14.1, could be used to estimate the size of an equivalent resistor network that adequately models these field data. The power law

$$\text{Var} = \text{size}^{0.55}, \quad (7)$$

which links the average distortion variance computed from random resistor networks to their number of cells [Bahr, 2000], has only been checked up to a network size of  $40 \times 40$ . If the same power law holds for larger network sizes, then a distortion variance of 14.1 corresponds to an equivalent network size of  $120 \times 120$  cells. Comparing the number of  $120 \times 120$  cells in the equivalent network to the size of the array in Figure 1,  $\sim 1000 \times 1000$  km suggest that a single cell or resistor represents an  $8 \times 8$  km area. This provides support for the assumption that the equivalent resistor network is in the vicinity of a percolation threshold where the distortion variance for a particular network size is maximal. Without this assumption, in order to explain the same field data an even larger resistor network with more resistors would be required, and this would result in the estimation of an even smaller area size. However, structures smaller than 8 km, although they certainly exist, cannot be resolved in the lower crust as deep as 30 km with electromagnetic volume sounding techniques.

[15] Independent support for the assumption that the equivalent resistor network is in the vicinity of a percolation threshold comes from a comparison of the overall scaling coefficients (equation (5)), calculated from field data, with those calculated from the network model. The distribution function of the overall scaling coefficients (equation (5)) created with the  $40 \times 40$  network is displayed in Figure 6. When plotted on a logarithmic scale, scaling coefficients within a wide range, 0.25–4 appear equally often, while scaling coefficients larger than 4 occur less often due to the limited size of the network. Scaling coefficients less than 0.125 appear more often due to the condition that the average  $a_{11}$  has to be 1 in the numerical experiment.

[16] The modeled distribution in Figure 6 does not match the field data distribution function in Figure 3 but only reproduces the broadness of the scaling coefficients from 0.125 to 16. In order to demonstrate that this broadness is also a consequence of extreme heterogeneity, two numerical experiments were performed:

1. We show the difference between the statistical magnetotelluric approach in this study, and a regional field experiment with small site spacing, with neighboring sites giving similar results. Resistor network experiments reproduce the distortion which we would find with a virtual  $40 \times 40$  cluster of MT sites at the depth of the middle crust,

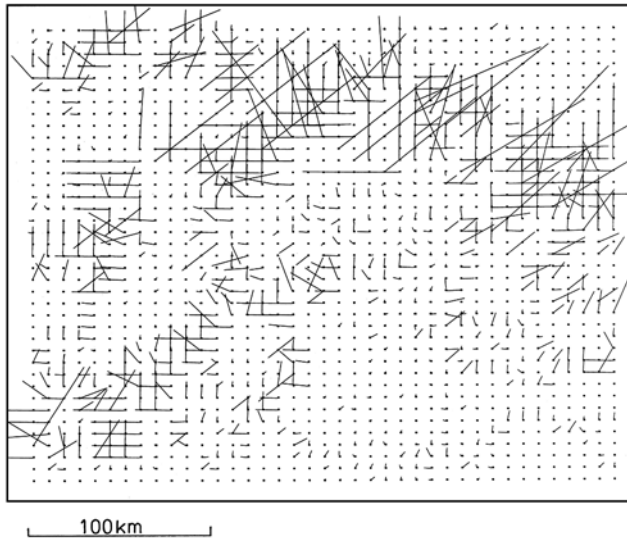


**Figure 5.** Distortion vectors according to equation (2) for 1521 sites of the network in Figure 4. Alternatively, this figure can also depict distortion vectors in a fraction of a random realization of the virtual  $120 \times 120$  resistor network that represents the lower crust of Fennoscandia (see Figure 4). A comparison with the field data in Figure 2 shows that only a limited field data sample has been collected.

situated on top of the heterogeneous structure. If a more homogenous upper crust is situated between this structure and the measurement sites, then we expect that neighboring sites give similar results and that therefore the distribution function is less broad. This effect can be simulated numerically by averaging the scaling coefficients over  $4 \times 4$  or  $9 \times 9$  neighboring cells (Figure 6), and the average distortion coefficient centers around 1.

2. We calculated a distribution function of modeled scaling coefficients for a  $40 \times 40$  resistor network that does

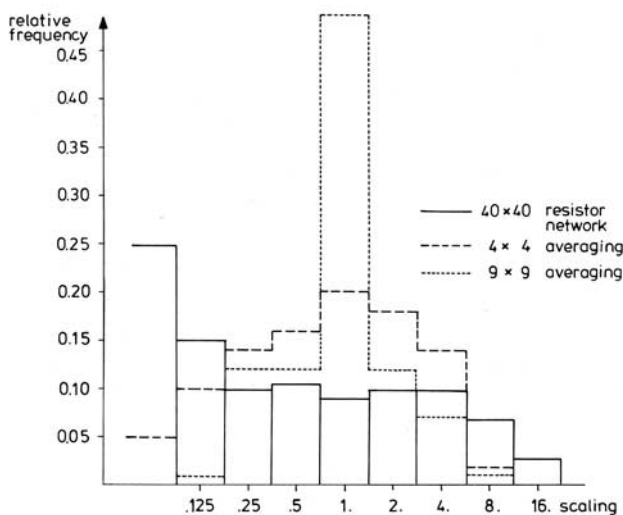


**Figure 6.** Frequency distribution of the dimensionless overall scaling coefficients according to equation (5) for 1521 sites of the resistor network in Figure 4. The dashed lines display the distribution functions of scaling coefficients that were averaged over 16 or 81 neighboring cells.

not stay close to the percolation threshold, e.g., 75% rather than 50% of the resistors represent the conductive phase. Again the broadness ceases and the resulting distribution function is close to the one obtained for the  $4 \times 4$  averaging in Figure 6.

[17] However, the form of the distribution function in Figure 6 does not match the skewed form of the field data distribution function in Figure 3. Therefore, in a third numerical experiment, we include “anisotropy” of the distribution of resistors representing the high conductive phase. Instead of allowing for 50% of those in both directions, we use 30% in the  $x$  direction and 70% in the  $y$  direction. The overall scaling coefficient distribution function is plotted in Figure 7, and it matches the field data, Figure 3, to some extent. In particular, in both distribution functions the median occurs at a scaling coefficient larger than 1. The 30%/70% fractions have been chosen because with a much smaller degree of anisotropy (e.g., 45%/55%) the distribution function would look much like the one of the isotropic network in Figure 6. With a much larger anisotropy the network would not be close to a percolation threshold anymore, as indicated by a decreased broadness of the distribution function. The match between field and model data is far from perfect due to the limited size of the field data sample, and possibly the implementation of anisotropy is too simplistic: in the real crust, the degree and direction with in the target area varies with location.

[18] In summary, the distortion variance and the broadness of the distribution function of the field data can be explained with a very heterogeneous random resistor network in the vicinity of the percolation threshold. The conductive phase of such a network has a fractal geometry [Labendz, 1999]. However, the fact that the statistical properties of the field data can be reproduced with a fractal model is not the proof that the deep Fennoscandian crust has a fractal geometry. There is other evidence, as shown in the discussion. The distribution function of the field data can be better reproduced if the random resistor network is anisotropic.

#### 4. Finding an Analogue Model That Supports Fractals

[19] There are many geological or tectonic processes that can generate fractal structures, e.g., folds or fractures. A

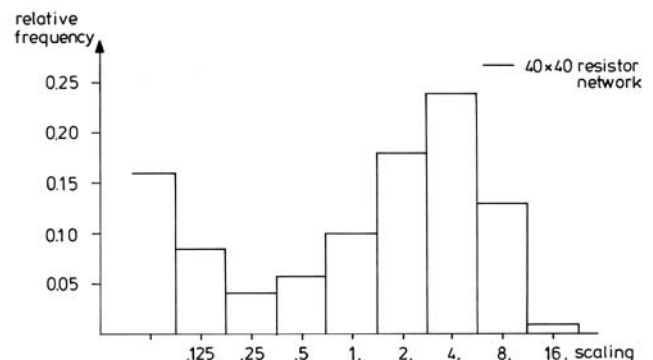


**Figure 7.** Frequency distribution of scaling coefficients according to equation (5) for 1521 sites of an anisotropic  $40 \times 40$  resistor network.

common definition of a fractal set is one with no characteristic length scale, but it does not describe these natural fractal sets, because they have natural upper and lower bounds [Bonnet *et al.*, 2001]. In section 3 we tried to show that magnetotelluric data collected in an area almost as large as Fennoscandia can provide some evidence that a fractal conductive structure exists with an upper bound as large as Fennoscandia. The search for a process that can generate this large structure leads to analogue models for crustal formation, which was first developed by Hubbart [1937]. Scheidegger [1956] pointed out that the “crustal” analogue material in the model has to be “weak” with respect to its shear modulus. We first repeat Scheidegger’s [1956] physical scaling model and then extend it in order to include viscosity. Suppose the length scaling factor is  $l = 5 \times 10^{-6}$ , e.g., the analogue model of the continental crust is 15–30 cm thick. Because the analogue material will have a density around  $1.5 \text{ g/cm}^3$  and the density scaling factor  $\rho = 0.5$  links the length scaling and the mass scaling  $m$  according to

$$\rho = m/l^3, \quad (8)$$

the mass scaling can be found to  $m = 6.25 \times 10^{-17}$ . Because the real and the analogue crust are subject to the same gravity force,

$$l/t^2 = 1, \quad (9)$$

the time scaling can be found to be  $2.24 \times 10^{-3}$ . The scaling factor for pressure is

$$p = m/(lt^2) = 2.5 \times 10^{-6}. \quad (10)$$

The pressure at the base of the crust,  $10^9$  Pa, translates to 2500 Pa in the model, and stress of this order of magnitude should be sufficient to deform the analogue material. “Butter would be much too strong” [Scheidegger, 1956, p. 272].

[20] Including viscosity into Scheidegger’s [1956] thought experiment yields a viscosity scaling factor

$$\eta = m/(lt) = 5 \times 10^{-9}. \quad (11)$$

The viscosity of the lower crust has been measured in laboratory studies [e.g., Rutter and Brodie, 1992] but has also been estimated in models of ductile flow [Kaufmann and Royden, 1994; Kruse *et al.*, 1991], and in most studies the result is in the  $10^{19}$ – $10^{21}$  Pa s range. The analog material in the thought experiment should therefore have a viscosity in the  $10^9$ – $10^{11}$  Pa s range. Butter would be too viscous and glycerin ( $\eta = 1$  Pa s) would be too fluid. Glucose at  $30^\circ\text{C}$  has a viscosity of  $10^{10}$  Pa s. The search for an analogue material for a particular piece of the middle crust which undergoes the ductile-brittle transition should also be joined by the search for an analogue process.

[21] Broderix *et al.* [1999] investigated the viscosity of a randomly cross-linked melt of phantom polymers during the process of gelation: the transition from a solution to gelatine. At the gelation transition a macroscopic cluster of polymers is formed, resulting in a divergence of the viscosity at the critical point and justifying its interpretation as a percolation transition [e.g., Stauffer *et al.*, 1982]. Broderix *et al.* [1999] analytically derive an exact relation between the viscosity and the resistances measured in a corresponding random resistor network. A realization of a random resistor network close to the percolation threshold

in Figure 4 can also be thought of a realization of the polymer melt at the gelation transition, where the black resistor clusters represent polymers which are already bound together. However, this does not imply an analogy between conductivity and viscosity. The similarity is limited to the occurrence of two modes in both fractal models, because polymer are either “still molten” or “already bound together” and in the network two types of resistors occur.

[22] Gelation of a two-phase mixture is suggested as a small-scale analogy for the process of crust formation. It can be described in three steps:

1. Before the gelation transition is approached from the solution side, the viscosity is very low. If conductive material is available, then it is distributed arbitrarily and a conductive network is not supported.

2. At the gelation transition, the host medium develops mechanically stable fractal structures, e.g., one macroscopic cluster and a fractal distribution of clusters on all smaller scales. If additional conductive material is available, it follows the geometry of these structures, and a fraction of this material forms a macroscopic conductive network. Again no analogy between conductivity and viscosity is set up because if gelatine would be used as actual analogue material, then an additional component would necessary to represent the conductive phase in the analogue model.

3. As the gelation continues beyond the critical point, the viscosity increases so strongly that movement of material is not possible, except through the development of cracks.

## 5. Discussion: Heterogeneity and Anisotropy—Gelation and Terrane Accretion

[23] Kozlovskaya and Hjelt [2000] stress the importance of model parametrization schemes that can be used to model the distribution of more than one physical parameter. They choose the fractal rock model because it allows the description of the real complicated rock microstructure by a relatively small number of parameters and because elastic and electric properties can be calculated within that framework. In this paper, we have shown that a statistical evaluation of field data can provide independent evidence that fractal structures might exist in parts of the crust.

[24] With respect to our modeling procedure, it is important to understand that this study differs in two ways from conventional EM studies. (1) The distortion of electromagnetic fields, which is normally referred to as “geological noise” and which is removed from the data prior to their interpretation, carries important information which is evaluated here. (2) “Modeling” does not mean that one particular model is considered that would reproduce the special distortion observed in our field data. Instead, statistical properties of the magnetotelluric distortion measured in a large sparse array have been compared to similar distortion measures modeled with random resistor networks. Reproducing the special distortion in these field data would require array measurements with an array of  $120 \times 120$  MT field sites, matching the size of the equivalent resistor network introduced in section 3. The first novel point of this study is that so many field sites are not necessary if only the degree of heterogeneity is to be examined.

[25] Fractals do occur frequently in the earth sciences now, but another novel point is that evidence for an electri-

cally conductive fractal structure with an upper bound of the size of Fennoscandia is provided. The field data support the model of these fractal structures in the lower crust in three independent ways:

1. Evidence comes from the distortion at individual sites: The size of the skew angles (equation (2)) and the appearance of large scaling coefficients (equation (3)) can be explained by the action of a network in the vicinity of the percolation threshold on the long-period electromagnetic field [Bahr, 2000].

2. In this paper, we provided independent evidence through the application of statistical magnetotellurics: The comparison of the distortion variance (equation (6)) from field data with the numerically generated power law for this parameter (equation (7)) showed that in an equivalent resistor network representing the Fennoscandian lower crust, each resistor represents a  $10 \text{ km} \times 10 \text{ km}$  area. A departure from the assumption that the network stays in the vicinity of the percolation threshold would lead to a smaller area and contradict the limited resolution of any electromagnetic diffusion process.

3. Again statistical magnetotellurics is employed in an attempt to show that the distribution function of the distortion parameters can best be explained with a combination of extreme heterogeneity and anisotropy (Figures 3 and 7).

[26] There are many other processes that create fractal structures, e.g., fluid percolation [Guéguen *et al.*, 1991] in self-similar crack networks [Schmittbuhl *et al.*, 1995; Meheust and Schmittbuhl, 2000]. There might also be different argumentative transitions than the one from heterogeneity to fractals, and the one from fractals to gelation. However, the gelation analogy offers a few advantages which other models do not have.

[27] The concept of “brittle” and “ductile” behavior of rocks explains laboratory measurements under different pressure and temperature regimes [Rutter and Brodie, 1992], but this explanation is, in most cases, limited to the laboratory scale. On a larger scale (10–30 km) deep earthquakes have been observed in Fennoscandia [Arvidsson and Kulhanek, 1994] (see also review by Simpson [1999, and references therein]), indicating that a simple ductile model of the lower crust is not adequate. This could be explained by a Maxwell (frequency-dependent) rheology similar to the rheology of the mantle, but the gelation analogy also explains the coexistence of ductile and brittle behavior over a long timescale. An example for this coexistence is the survival of two-phase structures over geological times, as indicated by the presence of fractal conductive structure in the lower crust of an old craton like Fennoscandia. The gelation analogy allows for a quick formation of the fractal structure because of the small time scaling,  $t = 2.24 \times 10^{-3}$ , which indicates that the process is “fast” compared to the timescale of ductile flow. In contrast, in an analogue model for geothermal diffusion processes, equation (9) would be replaced by

$$l^2/t = 1, \quad (12)$$

and therefore the length scale used in section 4 would translate into a timescale  $t = 2.5 \times 10^{-11}$  (10 Myr equivalent to 1 hour). While thermal cooling is a very slow

process, gelation is very quick. However, temperature plays, of course, an important role by controlling the onset of the process. According to Rutter and Brodie [1992], ductile flow and recrystallization can produce alignment of minerals, and this occurs over a wide range of pressure and temperature environments. The alignment might be related to electrical anisotropy, but the occurrence of that anisotropy is scale-dependent, as discussed below.

[28] Physical scaling was used for three reasons:

1. Scaling creates quantitative models of earth materials in large volumes that are inaccessible to laboratory studies, and provides a link between laboratory and geophysical field studies.

2. The viscosity of the analogue material is found to be  $10^{10}$ – $10^{12}$  Pa s, comparable to gelatine. However, the gelation analogy must not be overstretched. It was simply introduced because theoretical studies of the gelation process have provided evidence that is associated with the occurrence of fractal structures [Broderix *et al.*, 1999]. A more geological analogue material with a viscosity in the  $10^{10}$ – $10^{12}$  Pa s range would be granitic melt at 1050 K [Webb, 1997].

3. The time scaling factor of the crustal formation process is found to be small, indicating that this process is fast.

[29] The question whether geological structures are just very heterogeneous or, additionally, anisotropic with respect to electrical conductivity is related to the question whether tectonic evolution is a random process, and the answer depends on the scale of the structure:

[30] On the small scale (<10 km) magnetotelluric data cannot resolve any anisotropic structures at lower crustal depths. Laboratory measurements of borehole samples from the German deep drill hole KTB [Rauen and Lastovickova, 1995] yielded small (2.3) anisotropies. Large anisotropy found in magnetotelluric field data from the same area led to the model of originally randomly oriented cracks to which horizontal tectonic force are applied. If the geometry of the crack network is fractal, then a scale dependent anisotropy is found [Bahr, 1997]. In contrast, large (10–20) electrical anisotropy was found in hand samples from a former terrane boundary [Jones *et al.*, 1997], and inactive terrane boundaries can be a source of anisotropy in magnetotelluric field data.

[31] In magnetotelluric field studies carried out on an intermediate scale (50–300 km) with significantly smaller (<20 km) site spacing than in this study, electrical anisotropy has been found in the lower crust, and the direction of the high conductivity is parallel to paleoterrane boundaries [Bahr *et al.*, 2000, and references therein]. Because the anisotropy is also found at sites far away from terrane boundaries (the distance is larger than the electromagnetic penetration depth), it cannot only be related to small-scale anisotropy at the terrane boundaries. Heise and Pous [2001] demonstrate the effect of undetected anisotropy on the model results of two-dimensional inversions. Their results suggest that anisotropy occurs more often than hitherto assumed. Again a combination of a process which creates randomly oriented conductive structures and horizontal tectonic forces can create anisotropic conductive structures in the lower crust within the terrane. In Fennoscandia, crustal conductors have been found with regional magnetotelluric studies, and their orientation and size are to some



extent related to paleoterrane boundaries [Korja and Hjelt, 1993; Korja et al., 1993].

[32] The field data presented here have been collected in a 900 km × 900 km array. On this scale, many paleoterranes are part of the target area. Some of them have been identified, e.g., the Caledonian domain or the Karelian domain, but the 3 × 10<sup>9</sup> year old history of terrane accretion is not entirely known. Most likely, tectonic forces in many different directions were acting on “Fennoscandia” during different stages of its accumulation. Then MT data from the large sparse array with sites on many different paleoterranes do not resolve structure but a random distribution of directions.

[33] In summary, random processes play important roles: The gelation analogy suggested here as a hypothesis on the small and intermediate size, and terrane accretion over geological times on the very large scale. On the intermediate scale, tectonic events can result in conductivity structures that are certainly not random.

[34] **Acknowledgments.** Toivo Korja first suggested a large sparse electromagnetic array in Scandinavia, and acted as driving force for the BEAR experiment. We thank the 50 students, researchers, and guest field crew members who participated in the 1998 experiment. Gerda Schliebe and Rainer Hennings helped with the type setting and the figures. K.B. and E.St. acknowledge financial support from the German Science foundation under contract Ba 889/8 and M.S. acknowledges financial supports from INTAS.

[35] Note added in proof: We demonstrated that lower crustal conductivity structures can have a fractal geometry. Recently, Everett and Weiss [2002] showed that electromagnetic responses from near-surface structures can also be fractal signals.

## References

- Arvidsson, R., and O. Kulhanek, Seismodynamics of Sweden deduced from earthquake focal mechanisms, *Geophys. J. Int.*, **116**, 377–392, 1994.
- Bahr, K., Electrical anisotropy and conductivity distribution functions of fractal random networks and of the crust: The scale effect of connectivity, *Geophys. J. Int.*, **130**, 649–660, 1997.
- Bahr, K., Percolation in the crust derived from distortion of electric fields, *Geophys. Res. Lett.*, **27**, 1049–1052, 2000.
- Bahr, K., and A. Duba, Is the asthenosphere electrically anisotropic?, *Earth Planet Sci Lett.*, **178**, 87–95, 2000.
- Bahr, K., M. Bantín, C. Jantos, E. Schneider, and W. Storz, Electrical anisotropy from electromagnetic array data: Implications for the conduction mechanism and for distortion at long periods, *Phys. Earth Planet. Inter.*, **119**, 237–257, 2000.
- Bailey, R. J., J. A. Craven, J. C. Macnae, and B. D. Polzer, Imaging of deep fluids in Archean crust, *Nature*, **340**, 136–138, 1989.
- Bernasconi, J., Real-space renormalization of bond-disordered conductance lattices, *Phys. Rev. B*, **18**, 2185–2191, 1978.
- Bonnet, E., O. Bour, N. E. Odling, P. Davy, I. Main, P. Cowie, and B. Berkowitz, Scaling of fracture systems in geological media, *Rev. Geophys.*, **39**, 347–383, 2001.
- Broderix, K., H. Lowe, P. Müller, and A. Zippelius, Shear viscosity of a crosslinked polymer melt, *Europhys. Lett.*, **48**, 421–427, 1999.
- Everett, M. E., and C. J. Weiss, Geological noise in near-surface electromagnetic induction data, *Geophys. Res. Lett.*, **29**(1), 1010, doi:10.1029/2001GL014049, 2002.
- Groom, R. W., and K. Bahr, Corrections for near surface effects: Decomposition of the magnetotelluric impedance tensor and scaling corrections for regional resistivities: A tutorial, *Surv. Geophys.*, **13**, 341–379, 1992.
- Guéguen, Y., C. David, and P. Gavrilenko, Percolation networks and fluid transport in the crust, *Geophys. Res. Lett.*, **18**, 931–934, 1991.
- Heise, W., and J. Pous, Effects of anisotropy on the two-dimensional inversion procedure, *Geophys. J. Int.*, **147**, 610–621, 2001.
- Hubbart, K. M., Theory of scale models as applied to the study of geological structures, *Geol. Soc. Am. Bull.*, **48**, 1459–1520, 1937.
- Jones, A. G., Electrical conductivity of the continental lower crust, in *Continental Lower Crust*, edited by D. M. Fountain, R. J. Arculus, and R. W. Kay, pp. 81–143, Elsevier Sci., New York, 1992.
- Jones, A. G., T. J. Katsube, and P. Schwann, The longest conductivity anomaly in the world explained: Sulphides in fold hinges causing very high electrical anisotropy, *J. Geomagn. Geoelectr.*, **49**, 1619–1629, 1997.
- Kaufmann, P. S., and L. Royden, Lower crustal flow in an extensional setting: Constraints from the Halloran Hills region, eastern Mojave Desert California, *J. Geophys. Res.*, **99**, 15,723–15,739, 1994.
- Kemmerle, K., On the influence of local anomalies of conductivity at the Earth's surface on magnetotelluric data, *Acta Geodaet. Geophys. Montanist. Sci Hung.*, **12**, 177–181, 1977.
- Korja, T., Electrical conductivity distribution of the lithosphere in the central Fennoscandian Shield, *Precambrian Res.*, **64**, 85–108, 1993.
- Korja, T., and BEAR Working Group, Baltic electromagnetic array research: An overview, paper presented at the 15th Workshop on Electromagnetic Induction, Int. Assoc. of Geomagn. and Aeron., Cabo Frio, Brazil, 19–26 Aug. 2000.
- Korja, T., and S.-E. Hjelt, Electromagnetic studies in the Fennoscandia Shield—Electrical conductivity of Precambrian crust, *Phys. Earth Planet. Inter.*, **81**, 107–138, 1993.
- Korja, A., T. Korja, U. Luosto, and P. Heikkinen, Seismic and geoelectric evidence for collisional and extensional events in the Fennoscandian Shield—Implications for Precambrian crustal evolution, *Tectonophysics*, **219**, 129–152, 1993.
- Kozlovskaya, E., and S.-E. Hjelt, Modelling of elastic and electrical properties of solid-liquid rock system with fractal microstructure, *Phys. Chem. Earth, Part A*, **25**, 5–200, 2000.
- Kruse, S., M. McNutt, J. Phipps-Morgan, L. Royden, and B. Wernicke, Lithospheric extension near Lake Mead, Nevada: A model for ductile flow in the lower crust, *J. Geophys. Res.*, **96**, 4435–4456, 1991.
- Labendz, D., Zwei- und dreidimensionale Widerstandsnetzwerke zur Beschreibung des Leitfähigkeitsmechanismus in der mittleren Kruste, dissertation Fak. Phys., Univ. Göttingen, Göttingen, Germany, 1999.
- Larsen, J. C., Low frequency (0.1–6.0 cpd) electromagnetic study of deep mantle electrical conductivity beneath the Hawaiian islands, *Geophys. J. R. Astron. Soc.*, **43**, 17–46, 1975.
- Madden, T. R., Random networks and mixing laws, *Geophysics*, **41**, 1104–1125, 1976.
- Mareschal, M., W. S. Fyfe, J. Percival, and T. Chan, Grain-boundary graphite in Kapuskasing gneisses and implication for lower crustal conductivity, *Nature*, **357**, 674–676, 1992.
- Marquis, G., and R. D. Hyndman, Geophysical support for aqueous fluids in the deep crust: Seismic and electrical relationships, *Geophys. J. Int.*, **110**, 91–105, 1992.
- Meheust, Y., and J. Schmittbuhl, Flow enhancement of a rough fracture, *Geophys. Res. Lett.*, **27**, 2989–2992, 2000.
- Merzer, A. M., and S. L. Klempner, High electrical conductivity in a model lower crust with unconnected, conductive, seismically reflective layers, *Geophys. J. Int.*, **108**, 895–905, 1992.
- Ogawa, Y., and T. Uchida, A two-dimensional magnetotelluric inversion assuming Gaussian static shift, *Geophys. J. Int.*, **126**, 69–76, 1996.
- Osipova, L. L., S.-E. Hjelt, and L. L. Vanyan, Source field problems in northern parts of the Baltic Shield, *Phys. Earth Planet. Inter.*, **53**, 337–342, 1989.
- Ranganayaki, R. P., and T. R. Madden, Generalized thin sheet analysis in magnetotellurics: An extension of Price's analysis, *Geophys. J. R. Astron. Soc.*, **60**, 445–457, 1980.
- Rauen, A., and M. Lastovickova, Investigation of electrical anisotropy in the deep borehole KTB, *Surv. Geophys.*, **16**, 37–46, 1995.
- Rutter, E. H., and K. Brodie, Rheology of the lower crust, in *The Continental Lower Crust*, edited by D. M. Fountain, R. J. Arculus, and R. W. Kay, pp. 201–267, Elsevier Sci., New York, 1992.
- Scheidegger, A. E., Forces in the Earth's crust, in *Handbuch der Physik, Geophysik I*, edited by S. Fluegge, pp. 258–287, Springer-Verlag, New York, 1956.
- Schmittbuhl, J., F. Schmitt, and C. Scholz, Scaling invariance of crack surfaces, *J. Geophys. Res.*, **100**, 5953–5973, 1995.
- Schmucker, U., Regional induction studies: A review of methods and results, *Phys. Earth Planet. Inter.*, **7**, 365–378, 1973.
- Simpson, F., Stress and seismicity in the lower continental crust: A challenge to simple ductility and implications for electrical conductivity mechanisms, *Surv. Geophys.*, **20**, 201–227, 1999.
- Simpson, F., Fluid trapping at the brittle-ductile transition re-examined, *Geofluids*, **1**, 123–136, 2001.
- Simpson, F., and M. Warner, Coincident magnetotelluric, P-wave and S-wave images of the deep continental crust beneath the Weardale granite, NE England: Seismic layering, low conductance and implications against the fluids paradigm, *Geophys. J. Int.*, **133**, 419–434, 1998.
- Smirnov, M., V. Ismagilov, and BEAR Working Group, Investigation of the source influence on the results of magnetotelluric data robust processing for the period range of geomagnetic pulsations from the BEAR data, paper presented at the 15th Workshop on Electromagnetic Induction, Int. Assoc. of Geomagn. and Aeron., Cabo Frio, Brazil, 19–26 Aug. 2000.

- Sokolova, E., I. Varentsov, and BEAR Working Group, Investigation and elimination of the polar source distortions in the BEAR project transfer functions, paper presented at the 15th Workshop on Electromagnetic Induction, Int. Assoc. of Geomagn. and Aeron., Cabo Frio, Brazil, 19–26 Aug. 2000.
- Stauffer, D., and A. Aharony, *Introduction to Percolation Theory*, 2nd ed., Taylor and Francis, Philadelphia, Pa., 1992.
- Stauffer, D., A. Coniglio, and M. Adam, Gelation and critical phenomena, *Adv. Polym. Sci.*, 44, 103, 1982.
- Waff, H. S., Theoretical considerations on electrical conductivity in a partially molten mantle and implications for geothermometry, *J. Geophys. Res.*, 79, 4003–4010, 1974.
- Wannamaker, P. E., Comment on “The petrological case for a dry lower crust” by Bruce W.D. Yardley and John W. Valley, *J. Geophys. Res.*, 105, 6057–6064, 2000.
- Webb, S., Silicate melts: Relaxation, rheology, and the glass transition, *Rev. Geophys.*, 35, 191–218, 1997.
- Xu, Y., T. J. Shankland, and B. T. Poe, Laboratory-based electrical conductivity in the Earth’s mantle, *J. Geophys. Res.*, 105, 27,865–27,875, 2000.
- Yardley, B. W. D., and J. W. Valley, The petrological case for a dry lower crust, *J. Geophys. Res.*, 102, 12,173–12,185, 1997.
- Yardley, B. W. D., and J. W. Valley, Reply, *J. Geophys. Res.*, 105, 6065–6068, 2000.

---

K. Bahr and E. Steveling, Institut für Geophysik, Herzberger Landstr. 180, D-37075 Göttingen, Germany. (kbahr@uni-geophys.gwdg.de; estevel@uni-geophys.gwdg.de)

M. Smirnov, Institute of Physics, Ulyanovskaya 1, Petrodvorets, St. Petersburg, PC 198904, Russia. (msmirnov@pcland3.phys.spbu.ru)

BEAR Working Group, T. Korja, Geological Survey of Finland, Betonimiehenuja 4, FI-02151 Espoo, Finland. (toivo.korja@gsf.fi)